J. Am. Soc. Mass Spectrom. (2016) 27:1805–1812
DOI: 10.1007/s13361-016-1467-0

RESEARCH ARTICLE

Laser-Induced Acoustic Desorption Atmospheric Pressure Photoionization via VUV-Generating Microplasmas

Kevin Benham,[1] Robert Hodyss,[2]
Facundo M. Fernández,[1] Thomas M. Orlando[1,3]

[1]School of Chemistry and Biochemistry, Georgia Institute of Technology, 901 Atlantic Drive NW, Atlanta, GA 30332, USA
[2]Cryogenic Chemistry Laboratory, Jet Propulsion Laboratory, California Institute of Technology, Pasadena, CA 91109, USA
[3]School of Physics, Georgia Institute of Technology, 837 State Street, Atlanta, GA 30332, USA

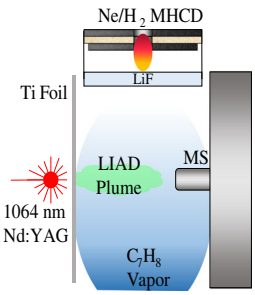

Abstract. We demonstrate the first application of laser-induced acoustic desorption (LIAD) and atmospheric pressure photoionization (APPI) as a mass spectrometric method for detecting low-polarity organics. This was accomplished using a Lyman-α (10.2 eV) photon generating microhollow cathode discharge (MHCD) microplasma photon source in conjunction with the addition of a gas-phase molecular dopant. This combination provided a soft desorption and a relatively soft ionization technique. Selected compounds analyzed include α-tocopherol, perylene, cholesterol, phenanthrene, phylloquinone, and squalene. Detectable surface concentrations as low as a few pmol per spot sampled were achievable using test molecules. The combination of LIAD and APPI provided a soft desorption and ionization technique that can allow detection of labile, low-polarity, structurally complex molecules over a wide mass range with minimal fragmentation.

Keywords: Laser-induced acoustic desorption, Atmospheric pressure photoionization, Microplasma, Microhollow cathode discharge, Low-polarity analytes

Received: 12 June 2016/Revised: 27 July 2016/Accepted: 28 July 2016/Published Online: 13 September 2016

Introduction

Over time, the field of mass spectrometry (MS) has expanded in scope because of the introduction of a variety of ion generation methods that extend the range of systems that can be probed. Of particular interest is the development of various MS techniques that are suitable to analyze minute amounts of analytes deposited on surfaces, each having different drawbacks and advantages [1]. Nonpolar molecules have, thus far, been difficult to analyze by surface MS techniques due to both the inherent ionization mechanisms and amount of energy imparted to the molecules during the desorption/ionization events. Owing to their low proton affinities, these compounds do not protonate easily, and are not detected with high sensitivity using techniques such as desorption electrospray ionization (DESI) or matrix-assisted desorption ionization (MALDI). As a consequence, alternative surface analysis techniques that focus on photoionization of neutral desorbates have been developed, including desorption atmospheric pressure photoionization (DAPPI) and laser ablation/desorption photoionization [2–4]. With DAPPI, a heated solvent jet desorbs analytes from a surface, which undergo atmospheric pressure photoionization (APPI) initiated by a radiofrequency-driven vacuum ultraviolet radiation (rF-VVU) emitting lamp and then swept into the atmospheric pressure inlet of a mass spectrometer. Despite its appealing coverage in terms of analyte polarity, studies have suggested DAPPI may not be best suited for labile high molecular weight compounds because of the relatively large amount of heat required to desorb larger molecules, and the subsequent fragmentation [5]. As for methods involving direct (without matrix) laser ablation/desorption, these are also known to produce fragmented gas-phase molecules because of direct irradiation from the desorption laser as well as above plume/plasma interactions. Direct laser ablation/desorption is also often limited to lower molecular weight desorbates [6].

Laser-induced acoustic desorption (LIAD) is capable of desorbing analytes in a wide range of molecular weights and has therefore received significant recent attention [7–10]. LIAD is accomplished by irradiating the backside of a metal foil ~ 5–20 μm thick with a nanosecond laser pulse of power density ~10^8 W/cm^2. After absorption of this pulse, molecular species are ejected from the opposite side of the foil with relatively little energy transferred to the desorbed species [11, 12]. Since LIAD is known to generate mostly neutral and intact molecules, this technique is well suited for softly producing

Correspondence to: Thomas Orlando;
e-mail: thomas.orlando@chemistry.gatech.edu

pulses of low-polarity thermally-labile gas-phase molecules [11, 13, 14]. Initial studies describing the LIAD process suggested an acoustic wave mechanism for volatilization [15]. However, subsequent studies suggest a more complex mechanism where laser-induced stresses in the foil cause cracks in deposited molecular crystals and repulsive non-equilibrium electronic surface states, thus creating desorption sites from which analytes are ejected [12, 16]. Though now considered to be misleading, we continue to use the term LIAD here due to familiarity. Applications of LIAD to ambient mass spectrometry surface analysis scenarios demonstrated its viability for desorption of various organic compounds in a mass range extending up to *m/z* 762 using atmospheric pressure chemical ionization (APCI) as the tool for ion generation [17].

Recent developments in microplasma ion sources for ambient/atmospheric MS have demonstrated their viability as vacuum ultraviolet (VUV) sources for APPI techniques [18]. This specific class of plasma device, the micro-hollow cathode discharge (MHCD), is characterized by a small hollow in the cathode of the device in which Pendel electrons experience multiple collisions with the plasma gas [19]. For a neon:hydrogen admixture discharge gas, these interactions are known to produce neon excimers that through near-resonant energy transfer dissociate H_2 leading to Lyman-α (10.2 eV) photon emission [20]. The emission spectra from these devices are also known to be dependent upon the discharge gas composition, flow rates, and discharge current/voltage [18, 21, 22].

In this work, the generation of VUV light and the potential utility of MHCDs as miniature, low power consumption, atmospheric pressure photoionization sources for applications in surface desorption measurements is demonstrated. Specifically, we report the first combination of LIAD and APPI for the analysis of low-polarity compounds deposited on titanium foil. This combination utilizes a MHCD with a LiF exit window that seals the plasma cavity, blocks the emission and release of reactive plasma species, and allows the transmission of VUV to mid-infrared photons. This LIAD-APPI approach provides the ability to detect picomoles of low-polarity substances on a foil surface, and is expected to be general and particularly applicable for larger molecules that are prone to unimolecular decay and fragmentation if desorbed by other means.

Experimental

Materials, Chemicals, and Sample Preparation

Titanium foil 12.7 μm thick (99.8% metals basis) for the LIAD experiments was purchased from Alfa Aesar (Ward Hill, MA, USA). The low-polarity compounds studied (α-tocopherol, perylene, cholesterol, phenanthrene, phylloquinone, and squalene), solvents (toluene, hexane, ethanol, dichloromethane), and molybdenum foil (100 μm thick) for the plasma device electrodes were purchased from Sigma Aldrich (St. Louis, MO, USA). The LiF window used in the MHCD device (10 mm diameter, 1 mm thick) was purchased from Crystran (Poole, Dorset, UK). Samples were deposited on the 12.7 μm Ti foil using the iMatrixSpray open source deposition system (Grubenacker, Switzerland). Solutions ranging from 10 mM to 1 μM were deposited by the iMatrixSpray system through 10 coating cycles, which leads to a pixel to pixel coefficient of variance of 7% or less [23].

Microplasma Device

The device developed for these experiments is a custom-built MHCD designed with a LiF window to ensure VUV photon transmission. The particular device used in this work (Figure 1) is an improved and miniaturized iteration of a previous device described by Symonds et al. [18]. Device diameter was scaled down by 35% and total volume was scaled down by 86% to ensure closer proximity of the MHCD output to the laser desorption/ionization region (Figure 2). As shown in Figure 1, the MHCD cathode and anode electrodes were separated by 100-μm-thick mica as a dielectric, and holes through the electrodes and mica spacer were fabricated between 100 and 200 μm in diameter by either mechanical drilling or electrical discharge machining. A ballast resistor (R = 97 kΩ) was used to limit the discharge current (Figure 1b).

Microplasma Operation

Lyman-α light (10.2 eV) generation was accomplished by operating the MHCD with the admixtures of 3%–7% hydrogen in neon as previously reported in similar devices [18]. For all mass spectrometry experiments, unless otherwise noted, a nitrogen purge in the device cavity (2 SLM) was allowed to run for 10 min and shut off before plasma ignition. The plasma gas mixture of 4% H_2 in Ne then flowed through the device at 40 sccm to enhance excimer formation and thus VUV emission [21]. Current delivered to the device was limited between 10 and 11 mA by the Stanford Research Systems model PS350 power supply (Sunnyvale, CA, USA). The corresponding applied voltages ranged between 1100 and 1200 V. Flow rates were controlled by two FMA-5500 series mass flow controllers (MFCs) from Omega Engineering (Stamford, CT, USA). For VUV energy-resolved spectroscopy experiments, the MHCD cavity was purged with argon and a 7% H_2 in Ne plasma gas flowed into the device at 70 sccm, while the current was varied between 5 and 10 mA. Though the VUV emission and LIAD-APPI experiments were carried out under slightly different relative gas mixing ratios, the emission is not expected to vary drastically, especially under constant current/discharge conditions.

VUV Monochromator Instrumentation

Measurements of the Lyman-α output of the device were made using a 0.2 m VUV monochromator (Acton VM-502) equipped with a sodium salicylate scintillator and photomultiplier tube detector at the Cryogenic Chemistry Laboratory at NASA's Jet Propulsion Laboratory (Pasadena, CA, USA). Calibration of the instrument was accomplished using a Hg lamp, and tuning of the

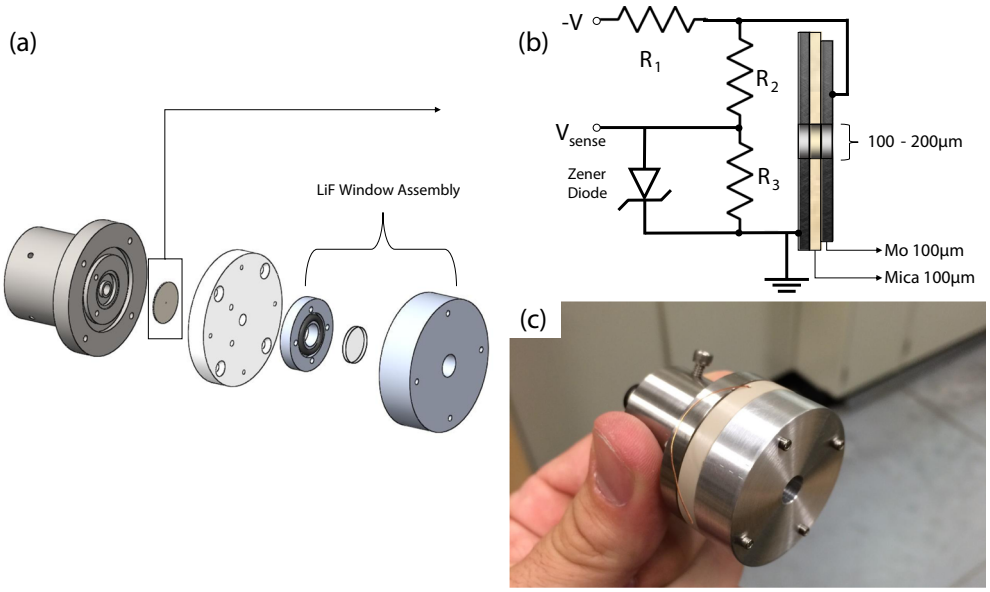

Figure 1. **(a)** Exploded view of the 3D model of the microplasma VUV device. **(b)** Circuit diagram with ballast resistor ($R_1 = 97$ kΩ) and voltage divider used for observing the discharge potential ($R_2 = 21$ MΩ, $R_3 = 560$ kΩ). **(c)** Picture of the device taken following fabrication

Lyman-α line resolution was performed with a rf argon/hydrogen lamp. Using the emission lines of Hg at 253.7 and 184.5 nm, a resolution of 5 Å could be estimated. For measurements on the plasma device, the spectrometer was operated at low vacuum (0.1 Torr) and the device was sealed to the monochromator inlet by Apiezon putty. This was done to reduce further attenuation of the Lyman-α emission intensity by windows external to the device.

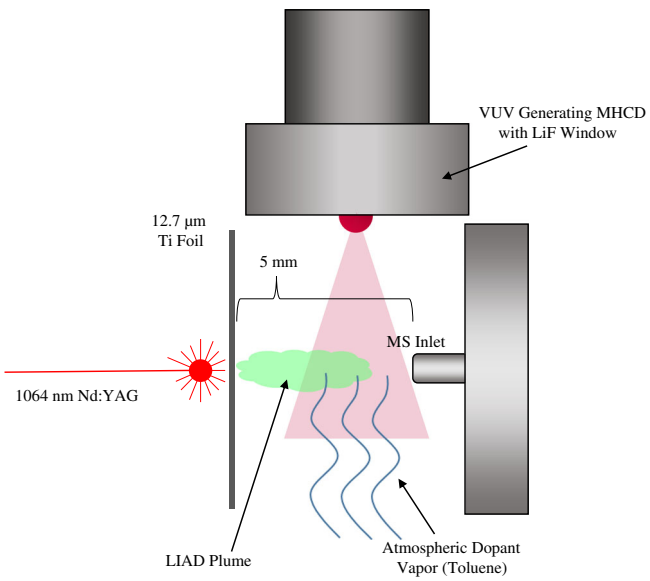

Figure 2. Schematic of the LIAD-APPI ion source assembly including a VUV-generating MHCD illustrating the process of desorbing molecules via LIAD, transferring them to the region containing reactive dopant photoions, and transfer into the mass spectrometer

LIAD-APPI Setup

The LIAD substrate foils were secured tightly over a metal tube to ensure a flat foil surface and placed at a fixed position 5 mm from the inlet of a Bruker micrOTOF-Q II mass spectrometer (Bruker, Billerica, MA, USA). The instrument was operated in positive mode in the range of 50 to 1000 *m/z* with the following settings: +50 V capillary bias, –50 V end plate offset, 3.0–4.0 L min^{-1} N_2 dry gas at 34 °C, 3.3 mbar foreline pressure, and a 5.81×10^{-7} mbar TOF pressure. A vial of high pressure liquid chromatography grade toluene was placed beneath the LIAD foil surface where the vapor present due to normal evaporative loss would act as an APPI dopant. The liquid level was checked and replenished periodically to ensure a consistent atmospheric concentration between experiments. A 1064 nm Nd:YAG laser (Continuum, San Jose, CA, USA) with a spot size of 0.11 cm^2 was aligned directly with the mass spectrometer inlet capillary at a power density of 0.6×10^8 W/cm^2, and operated at a pulse frequency of 10 Hz. This laser strikes the backside of the foil, ejecting molecules via the LIAD process into the region containing toluene photoions generated by Lyman-α photons from the MHCD. These molecules are then ionized via APPI mechanisms near and flowing towards the inlet of the mass spectrometer and are then collected. This process is schematically shown in Figure 2. Before all experiments, the MHCD was on with toluene present and signal was monitored. Base peak intensity from toluene oxidation products was observed to be between 1 and 1.5×10^4 counts and only significantly deviated from that amount if the photon producing discharge was observed to be unstable. Typical compound analyses were accomplished by taking 1 min of spectra in the 50–800 mass range, starting the laser pulse sequence after 6 s of collection with only the MHCD running. This length of data acquisition was done to observe signal rise time and signal consistency over time. Cholesterol and

α-tocopherol were studied in decreasing surface concentrations by depositing more dilute solutions of each on foil via the iMatrixSpray system.

Results and Discussion

Microplasma Lyman-α Output

The results for Lyman-α emission from the MHCD device are shown in Figure 3. The flow rate and hydrogen concentration used were held constant to observe the effect of plasma current on the output of the device. For the operating conditions described, Lyman-α flux was found to be greatest at a discharge current of 10 mA, which corresponds to an applied voltage of –1130 V. Though Lyman-α emission from MHCDs is known, it was important to assess generation and transmission through the LiF window for our particular device. Previous reports of these devices typically have them operating at pressures below 1 atm [20, 24, 25]. This demonstrates that Lyman-α can be successfully generated in the relatively high-pressure environment of our device and transmitted through the LiF window for photoionization use. Benefits of using this device include a compact, low power consumption alternative for generating Lyman-α. It is shown here to be generated at as low as 7 mA corresponding to 5.8 W of power consumption compared with 20–100 W consumption by typical Lyman-α rf VUV lamps. The emission from MHCDs is also known to be relatively more efficient because of the hollow cathode geometry increasing the density of high energy electrons and leading to efficient excimer formation [22]. Also, MHCDs do not require a high voltage spark source to initiate plasma breakdown because of the low breakdown voltage achieved by using a 100 μm electrode spacing and a 760 Torr operating pressure. This brings the value of the pressure-distance scaling to be at or near a minimum along the Paschen breakdown curve [26]. As mentioned previously, the potential for MHCDs to be tunable

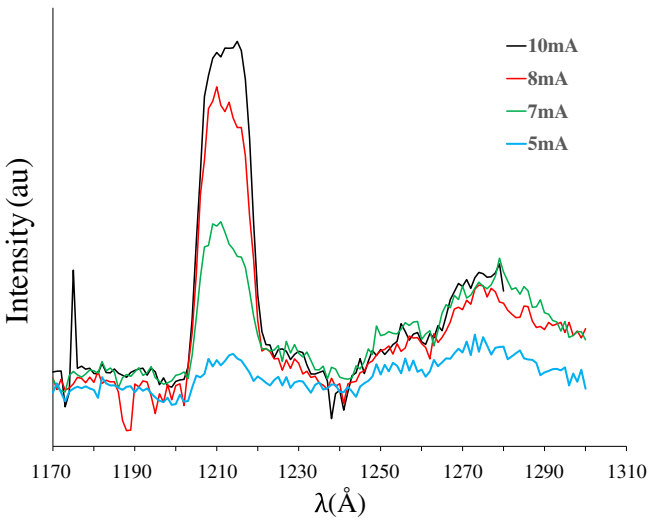

Figure 3. Measurements of Lyman-α emission at 1216 Å from the MHCD at varied discharge currents

photon sources also exists due to the observed spectral dependence on gas composition, plasma gas flow, and applied current/voltage [18, 21, 22]. With this in mind, it is conceivable that a set of operating parameters can be determined allowing for tunable emission spectra to rapidly alter emission spectra to desired photon energies for photoionization purposes. In conjunction with carefully selected dopants according to their ionization potentials (IPs), this could lead to a minimally energetic form of APPI.

LIAD-APPI of Low-Polarity Organics

To extend the applications of microplasmas in MS and to demonstrate a novel means for desorption and mass analysis of low-polarity species, α-tocopherol, perylene, cholesterol, phenanthrene, phylloquinone, and squalene were chosen for analysis by LIAD-APPI. For demonstration purposes, these analytes were deposited on the titanium foil in surface coverages of 10 nmol/cm^2. Control analyses were performed by recording spectra without the MHCD operating and laser firing. In every case, no analyte signal was observed. This may be due to absorption by atmospheric water dropping the 10.2 eV photon flux by two orders of magnitude over a few centimeters in the region of the LIAD plume combined with the neutral number density of desorbates being too low to yield any appreciable amount of photoionized products. Thus, the production and transport of toluene photoions within and towards the LIAD plume region has significant impact on ionization efficiency.

Resulting mass spectra taken in positive mode are shown in Figure 4. Interesting features of these spectra included relatively few species observed, dominated by the molecular ion for phenanthrene, perylene, α-tocopherol, and squalene, whereas the cholesterol spectra favored the $[M - H_2O]^+$ (*m/z* 368) and $[M - OH]^+$ (*m/z* 369) peaks and exhibited a weak signal from the $M^{+\cdot}$ (*m/z* 386). The presence of the $[M - H_2O]^+$ peak from cholesterol has been observed before in early electron impact studies where the mechanism of its formation was suggested to be complicated [27]. Phylloquinone was also successfully analyzed presenting a $[M + H]^+$ base peak at *m/z* 451. Spectra from α-tocopherol, cholesterol, and phylloquinone were also consistent with spectra reported in studies using DAPI and toluene as a dopant [5]. These results indicate LIAD-APPI is successful at desorbing and ionizing low-polarity organics, a class of molecules best suited to analysis by methods that do not owe their mechanism of ionization primarily to proton transfer. As a comparison, LIAD and synchrotron VUV photoionization have been combined previously under vacuum conditions to analyze heavy oils and lanthanide phthalocyanines extending up to *m/z* 1865 [9]. Our analysis approach should allow for higher sample throughput and a much easier and cost-effective method of photoionization in an atmospheric pressure setting.

Mechanisms of LIAD-APPI and Detection Limits

Mechanisms of APPI contributing to the effective ionization of low-polarity molecules desorbed via LIAD may include direct

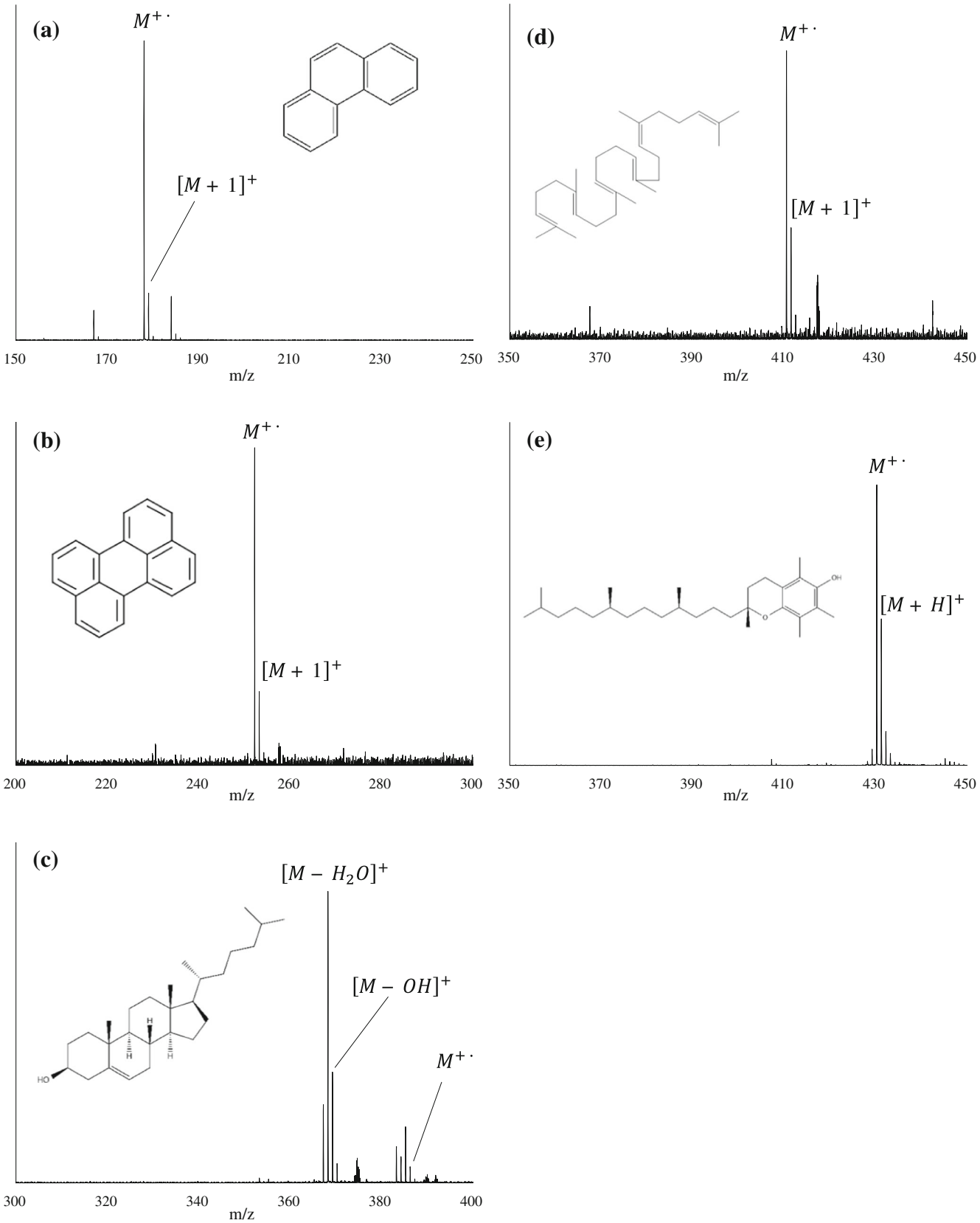

Figure 4. Positive ion mode spectra of phenanthrene **(a)**, perylene **(b)**, cholesterol **(c)**, squalene **(d)**, and α-tocopherol **(e)**. Indicated masses are $M^{+\cdot}$ at *m/z* 178, $[M + 1]^+$ at *m/z* 179 for **(a)**; $M^{+\cdot}$ at *m/z* 252, $[M + 1]^+$ at *m/z* 253 for **(b)**; $[M - H_2O]^+$ at *m/z* 368, $[M - OH]^+$ at *m/z* 369, $M^{+\cdot}$ at *m/z* 386 for **(c)**; $M^{+\cdot}$ at *m/z* 410, $[M + 1]^+$ at *m/z* 411 for **(d)**; and $M^{+\cdot}$ at *m/z* 430, $[M + H]^+$ *m/z* 431 for **(e)**

Table 1. Lowest Detected Amounts of Cholesterol and α-tocopherol. Foil Coverage Values were Calculated Using Parameters from the iMatrixSpray System and Relative Error Based on Inhomogeneity of Sample and Uncertainty in Laser Spot Size

Compound	Representative Peak	Solution Concentration [μM]	Foil Coverage (pmol/cm)	Lowest Detected Amount (pmol/spot)	Relative Error (±pmol/spot)
cholesterol	*m/z* 368 $[M - H_2O]^+$, *m/z* 369 $[M - OH]^+$	8.3	8.3	9.2	±2.8
α-tocopherol	*m/z* 430 $M^{+\cdot}$	2.7	2.7	3.0	±0.9

photoionization of the analyte, charge exchange with photoionized dopant molecules introduced in the sample region when the IP of the dopant is greater than that of the analyte, and protonation of higher proton affinity analytes via reactive dopant photoions [28]. No signal was observed in the absence of the toluene dopant, which is consistent with the observation that analyte ion-formation is heavily dependent upon the ion-molecule reactions with dopant photoions [28, 29]. Owing to the relatively low IP of toluene (IP = 8.8 eV) compared with other high vapor pressure dopant molecules [e.g., chlorobenzene and acetone (IP ≥ 9 eV)], we expect this to be a relatively soft means of charge transfer ionization [30–32]. The efficient formation of the molecular radical cation for the samples shown can be attributed to their effective ionization potentials. For α-tocopherol, phenanthrene, perylene, and squalene with IPs equal to 6.7 eV, 7.9 eV, 6.96 eV, and 6.9 eV, respectively, it can be concluded that the molecular radical cation peak is dominant due to all IPs being lower than that of toluene by at least 0.9 eV [33–36]. This allows for a very favorable charge exchange. With cholesterol (IP = 8.5 eV) and phylloquinone (estimated IP = ~9.3 eV compared with IPs of vitamin K2 derivatives), the IPs lie closer to or exceed that of toluene. This leads to reduced analyte ion formation from the charge exchange reaction [37, 38]. Early studies on cholesterol fragmentation support this observation using electron ionization at 70 and 16 eV, where the molecular radical cation was found to be the dominant peak in the mass spectrum and also demonstrates its sensitivity to internal vibrational temperature causing increased fragmentation [27, 39].

Estimating the toluene number density in the air to be ~10^{16} mL^{-1} due to vapor diffusion and using a cross section of 3.0×10^{-17} cm^2 for 10.2 eV toluene photoionization [40], the number density of toluene photoions can be estimated to be on the order of 10^5–10^6 mL^{-1}. This assumes a Lyman-α flux of 2.0×10^9 photons $s^{-1}sr^{-1}$ from an estimated 5% of total radiative output seen in Lyman-α lamps [18, 41]. This number is much smaller than the estimated number density of the desorbed products $N_{des} > 10^9$ mL^{-1}. This estimate assumes an average uniform upper bound for the toluene photoion density in the region of the LIAD plume, whereas the actual photoion density may be localized about the window of the MHCD, thus reducing the number density in the region of the plume even further. Thus, the sensitivity for this source geometry is enhanced by the forward scattering of the desorbates through the LIAD process and the pressure-driven flow at the inlet of the mass spectrometer but limited by the amount of toluene ions present lowering the ionization efficiency. Optimizing the setup to maximize collection consisted of observing base peak intensity of α-tocopherol spectra versus foil distance from the inlet. The result led to an optimum distance of 5 mm relative to the mass spectrometer sampling port. The higher collection at the optimum distance is mainly attributed to closer proximities cutting off photon flux, thereby reducing ions generated and further distances being too far for most desorbates to reach the inlet.

Owing to the unknown amount of analyte desorbed by each individual laser shot, we report the amount detected to be the initial amount present on an area the size of the laser beam diameter. This area was determined by observing the spatial disturbance of more concentrated films. To assess the sensitivity of the technique, representative samples of cholesterol and α-tocopherol were deposited in decreasing amounts on titanium foil to observe the lowest detectable amount of analyte per spot sampled. These molecules were chosen because of the ease with which they could be deposited in uniform coatings via the deposition method described above. The peaks used to determine the lowest detectable amounts were chosen by observing the base peaks from the demonstrative spectra. Choosing a signal to noise ratio of 3 for the peaks monitored to be considered detectable, the lowest detected amounts correspond to 9.2 pmol for cholesterol and 3.0 pmol for α-tocopherol. The results shown in Table 1 demonstrate that the technique is sensitive enough to observe few pmol quantities for the compounds chosen. These values are at or slightly lower than lowest corresponding molar amounts reported in DAPPI studies; however, an estimated limit-of-detection of 190 fmol for α-tocopherol with DAPPI has been reported [5, 42]. Improvements to obtain similar values such as using atmospheric dopant sprays to aid in desorbate transport and increase toluene photoion number density in the plume region are currently being explored. This would retain the known ability to softly desorb large molecular weight species with LIAD and aid in their atmospheric transport and ionization without overheating the sample. Overall, the results clearly indicate the potential for LIAD-APPI to be a highly sensitive technique for the analysis of low-polarity organics under ambient conditions.

Conclusion

The first application of laser-induced acoustic desorption and atmospheric pressure photoionization as a mass spectrometric method for detecting adsorbed low-polarity organic molecules has been demonstrated. The unique approach involved the use of a Lyman-α generating microhollow cathode discharge microplasma photon source in conjunction with the addition of a gas-phase molecular dopant. This combination provides both a soft desorption method and a relatively soft ionization

technique. The total energy inherent in the desorption step is low and the total energy deposited in the product ion is low enough to produce spectra with minimal fragmentation for most molecules. Detectable surface concentrations as low as a few pmol per spot were achievable using test molecules such as α-tocopherol and cholesterol. Efforts are underway to improve the ion transport and toluene photoion density parameters, which should extend the mass range to higher molecular weights and allow detection of lower concentrations than shown here. These include the use dopant sprays to aid in transport and increase ionization efficiency of molecules while still using LIAD as the main desorption mechanism. The sample preparation and analysis technique together may prove to be useful in detecting reaction products generated from drying aerosol sprays on metal surfaces. If successful, LIAD-APPI may prove to be a useful approach to detecting larger and more labile molecules, molecular assemblies, and aggregates than shown here.

Acknowledgments

This work was jointly supported by NSF and the NASA Astrobiology Program, under the NSF Center for Chemical Evolution, CHE-1504217. Work at JPL on VUV detection was supported by a joint Jet Propulsion Laboratory-Georgia Institute of Technology Strategic University Research Partnership (JPL-GIT SURP) grant.

References

1. Monge, M.E., Harris, G.A., Dwivedi, P., Fernandez, F.M.: Mass spectrometry: recent advances in direct open air surface sampling/ionization. Chem. Rev. **113**, 2269–2308 (2013)
2. Haapala, M., Pól, J., Saarela, V., Arvola, V., Kotiaho, T., Ketola R.A., Franssila, S., Kauppila, T.J., Kostiainen, R.: Desorption atmospheric pressure photoionization. Anal. Chem. **79**, 7867–7872 (2007)
3. Vaikkinen, A., Shrestha, B., Kauppila, T.J., Vertes, A., Kostiainen, R.: Infrared laser ablation atmospheric pressure photoionization mass spectrometry. Anal. Chem. **84**, 1630–1636 (2012)
4. Johnson, P.V., Hodyss, R., Beauchamp, J.L.: Ion funnel augmented Mars atmospheric pressure photoionization mass spectrometry for in situ detection of organic molecules. J. Am. Soc. Mass Spectrom. **25**, 1832–1840 (2014)
5. Suni, N.M., Aalto, H., Kauppila, T.J., Kotiaho, T., Kostiainen, R.: Analysis of lipids with desorption atmospheric pressure photoionization-mass spectrometry (DAPPI-MS) and desorption electrospray ionization-mass spectrometry (DESI-MS). J. Mass Spectrom. **47**, 611–619 (2012)
6. Wu, C., Dill, A.L., Eberlin, L.S., Cooks, R.G., Ifa, D.R.: Mass spectrometry imaging under ambient conditions. Mass Spectrom. Rev. **32**, 218–243 (2013)
7. Golovlev, V.V., Allman, S.L., Garrett, W.R., Chen, C.H.: Laser-induced acoustic desorption of electrons and ions. Appl. Phys. Lett. **71**, 852 (1997)
8. Sezer, U., Wörner, L., Horak, J., Felix, L., Tüxen, J., Götz, C., Vaziri, A., Mayor, M., Arndt, M.: Laser-induced acoustic desorption of natural and functionalized biochromophores. Anal. Chem. **87**, 5614–5619 (2015)
9. Jia, L., Weng, J., Zhou, Z., Qi, F., Guo, W., Zhao, L., Chen, J.: Note: Laser-induced acoustic desorption synchrotron vacuum ultraviolet photoionization mass spectrometry for analysis of fragile compounds and heavy oils. Rev. Sci. Instrum. **83**, 026105 (2012)
10. Cheng, S., Cheng, T.-L., Chang, H.-C., Shiea, J.: Using laser-induced acoustic desorption/electrospray ionization mass spectrometry to characterize small organic and large biological compounds in the solid state and in solution under ambient conditions. Anal. Chem. **81**, 868–874 (2009)
11. Pérez, J., Ramírez-Arizmendi, L.E., Petzold, C.J., Guler, L.P., Nelson, E.D., Kenttämaa, H.I.: Laser-induced acoustic desorption/chemical ionization in Fourier-transform ion cyclotron resonance mass spectrometry. Int. J. Mass Spectrom. **198**, 173–188 (2000)
12. Zinovev, A.V., Veryovkin, I.V., Moore, J.F., Pellin, M.J.: Laser-driven acoustic desorption of organic molecules from back-irradiated solid foils. Anal. Chem. **79**, 8232–8241 (2007)
13. Shea, R.C., Petzold, C.J., Liu, J.-A., Kenttämaa, H.I.: Experimental investigations of the internal energy of molecules evaporated via laser-induced acoustic desorption into a Fourier transform ion cyclotron resonance mass spectrometer. Anal. Chem. **79**, 1825–1832 (2007)
14. Reid, G.E., Tichy, S.E., Perez, J., O'Hair, R.A.J., Simpson, R.J., Kenttämaa, H.I.: N-terminal derivatization and fragmentation of neutral peptides via ion-molecule reactions with acylium ions: toward gas-phase edman degradation? J. Am. Chem. Soc. **123**, 1184–1192 (2001)
15. Linder, B., Seydel, U.: Laser desorption mass spectrometry of nonvolatlles under shock wave conditions. Anal. Chem. **57**, 895–899 (1985)
16. Zinovev, A.V., Veryovkin, I.V., Pellin, M.J., Iguchi, T., Watanabe, K.: Laser-induced desorption of organic molecules from front- and back-irradiated metal foils. Proc. AIP Conf. **1104**, 200–206 (2009)
17. Nyadong, L., McKenna, A.M., Hendrickson, C.L., Rodgers, R.P., Marshall, A.G.: Atmospheric pressure laser-induced acoustic desorption chemical ionization Fourier transform ion cyclotron resonance mass spectrometry for the analysis of complex mixtures. Anal. Chem. **83**, 1616–1623 (2011)
18. Symonds, J.M., Gann, R.N., Fernandez, F.M., Orlando, T.M.: Microplasma discharge vacuum ultraviolet photoionization source for atmospheric pressure ionization mass spectrometry. J. Am. Soc. Mass Spectrom. **25**, 1557–1564 (2014)
19. Günther-Schulze, A.: Die Stromdichte des Normalen Kathodenfalles. Z. Phys. **19**, 313–332 (1923)
20. Kurunczi, P.F., Shah, H., Becker, K.H.: Hydrogen Lyman-alpha and Lyman-beta emissions from high-pressure microhollow cathode discharges in Ne–H2 mixtures. J. Phys. B **32**, L651–L658 (1999)
21. Moselhy, M., Petzenhauser, I., Frank, K., Schoenbach, K.H.: Excimer emission from microhollow cathode discharges. J. Phys. D **36**, 2922–2927 (2003)
22. Becker, K.H., Kurunczi, P.F., Schoenbach, K.H.: Collisional and radiative processes in high-pressure discharge plasmas. Phy. Plasmas **9**, 2399 (2002)
23. Stoeckli, M., Staab, D.: Reproducible matrix deposition for MALDI MSI based on open-source software and hardware. J. Am. Soc. Mass Spectrom. **26**, 911–914 (2015)
24. Wieser, J., Salvermoser, M., Shawy, L.H., Ulrich, A., Murnick, D.E., Dahiz, H.: Lyman-alpha emission via resonant energy transfer. J. Phys. B **31**, 4589–4597 (1998)
25. Kurunczi, P.F., Martus, K.E., Becker, K.H.: Neon excimer emission from pulsed high-pressure microhollow cathode discharge plasmas. Int. J. Mass Spectrom. **223/224**, 37–43 (2003)
26. Paschen, F.: Ann. Phys. **273**, 69–96 (1889)
27. Wyllie, S.G., Amos, B.A., Tökés, L.: Electron impact induced fragmentation of cholesterol and related C-5 unsaturated steroids. J. Org. Chem. **42**, 725–732 (1977)
28. Kauppila, T.J., Kuuranne, T., Meurer, E.C., Eberlin, M.N., Kotiaho, T., Kostiainen, R.: Atmospheric pressure photoionization mass spectrometry. Ionization mechanism and the effect of solvent on the ionization of naphthalenes. Anal. Chem. **74**, 5470–5479 (2002)
29. Robb, D.B., Covey, T.R., Bruins, A.P.: Atmospheric pressure photoionization: an ionization method for liquid chromatography-mass spectrometry. Anal. Chem. **72**, 3653–3659 (2000)
30. Lu, K.-T., Eiden, G.C., Weisshaar, J.C.: Toluene cation: nearly free rotation of the methyl group. J. Phys. Chem. **96**, 9742–9748 (1992)
31. Baer, T., Tsai, B.P., Smith, D., Murray, P.T.: Absolute unimolecular decay rates of energy selected metastable halobenzene ions. J. Chem. Phys. **64**, 2460–2465 (1976)
32. Traeger, J.C., McLouglin, R.G., Nicholson, A.J.C.: Heat of formation for acetyl cation in the gas phase. J. Am. Chem. Soc. **104**, 5318–5322 (1982)
33. Klein, E., Lukeš, V., Ilčin, M.: DFT/B3LYP study of tocopherols and chromans antioxidant action energetics. Chem. Phys. **336**, 51–57 (2007)
34. Thantu, N., Weber, P.M.: Dependence of two-photon ionization photoelectron spectra on laser coherence band width. Chem. Phys. Lett. **214**, 276–280 (1993)
35. Shchuka, M.I., Motyka, A.L., Topp, M.R.: Two-photon threshold ionization spectroscopy of perylene and Van der Waals complexes. Chem. Phys. Lett. **164**, 87–95 (1989)
36. Koizumi, H., Lacmann, K., Schmidt, W.F.: VUV light-induced electron emission from organic liquids. J. Electron. Spectrosc. Relat. Phenom. **67**, 417–427 (1994)

37. Novak, I., Kovac, B.: Electronic structure and biological activity of steroids. Biophys. Chem. **78**, 233–240 (1999)
38. Ishihara, M., Sakagami, H.: QSAR of molecular structure and cytotoxic activity of vitamin K2 derivatives with concept of absolute hardness. Anticancer Res. **27**, 4059–4064 (2007)
39. Amirav, A.: Electron impact mass spectrometry of cholesterol in supersonic molecular beams. J. Phys. Chem. **94**, 5200–5202 (1990)
40. Zhou, Z., Xie, M., Wang, Z., Qi, F.: Determination of absolute photoionization cross-sections of aromatics and aromatic derivatives. Rapid Commun. Mass Spectrom. **23**, 3994–4002 (2009)
41. Cottin, H., Moore, M.H., Bénilan, Y.: Photodestruction of relevant interstellar molecules in ice mixtures. Astrophys. J. **590**, 874–881 (2003)
42. Räsänen, R.-M., Dwivedi, P., Fernández, F.M., Kauppila, T.J.: Desorption atmospheric pressure photoionization and direct analysis in real time coupled with travelling wave ion mobility mass spectrometry. Rapid Commun. Mass Spectrom. **28**, 2325–2336 (2014)